Report

Current Biology

Petal-shaped femoral lobes facilitate gliding in orchid mantises

Graphical abstract

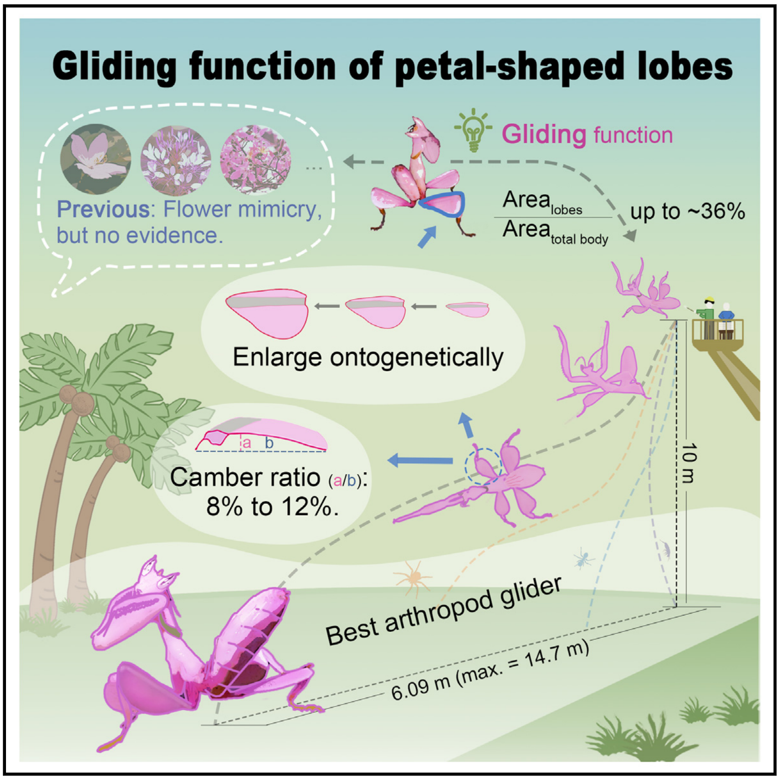

Highlights

- Orchid mantis nymphs achieve the best average glide angles across arthropods
- The petal-shaped femoral lobes are cambered airfoils, likely facilitating gliding
- The four femoral lobes increase the total planform area of the mantis by 20%–36%
- Body size growth did not compromise gliding, likely due to lobe enlargement

Authors

Xin Zhao, Jing-Xin Liu,
Tristan Charles-Dominique, ...,
James C. O'Hanlon, Yu Zeng,
Zhanqi Chen

Correspondence

zeng@berkeley.edu (Y.Z.),
chenzhanqi@xtbg.ac.cn (Z.C.)

In brief

Zhao et al. show that the petal-shaped lobes in orchid mantises function to facilitate gliding. These lobes are the first documented rigid exoskeletal structures for gliding, enabling orchid mantises to be the best arthropod gliders documented to date. This implies that gliding could be one force driving the evolution of flat extensions in arthropods.

Zhao et al., 2024, Current Biology *34*, 183–189
January 8, 2024 © 2023 Elsevier Inc.
https://doi.org/10.1016/j.cub.2023.11.003

Current Biology

CellPress

Report

Petal-shaped femoral lobes facilitate gliding in orchid mantises

Xin Zhao,[1,2] Jing-Xin Liu,[1] Tristan Charles-Dominique,[3,4] Ahimsa Campos-Arceiz,[5,6] Bing Dong,[7] Lin Yan,[8] James C. O'Hanlon,[9] Yu Zeng,[10,11,*] and Zhanqi Chen[1,11,12,*]
[1]Key Laboratory of Tropical Forest Ecology, Xishuangbanna Tropical Botanical Garden, Chinese Academy of Sciences, Yunnan 666303, China
[2]University of Chinese Academy of Sciences, Beijing 100049, China
[3]CNRS UMR5120, UMR AMAP, University Montpellier, CIRAD, CNRS, INRAE, IRD, Montpellier 34980, France
[4]CNRS UMR7618, Sorbonne University, Institute of Ecology and Environmental Sciences, 4 Place Jussieu, Paris 75005, France
[5]Center for Integrative Conservation, Xishuangbanna Tropical Botanical Garden, Chinese Academy of Sciences, Yunnan 666303, China
[6]Southeast Asia Biodiversity Research Institute, Xishuangbanna Tropical Botanical Garden, Chinese Academy of Sciences, Yunnan 666303, China
[7]School of Biology, University of St Andrews, Dyers Brae, St Andrews KY16 9TH, UK
[8]Department of Environmental Science, Policy and Management, University of California, Berkeley, Berkeley, CA 94720-3114, USA
[9]Armidale, NSW 2350, Australia
[10]Department of Integrative Biology, University of South Florida, Tampa, FL 33620, USA
[11]These authors contributed equally
[12]Lead contact
*Correspondence: zeng@berkeley.edu (Y.Z.), chenzhanqi@xtbg.ac.cn (Z.C.)
https://doi.org/10.1016/j.cub.2023.11.003

SUMMARY

To glide in forest canopies, arboreal vertebrates evolved various skin-derived aerodynamic structures, such as patagial membranes or webbing, but no comparable structure has been reported from wingless arboreal arthropods.[1–3] Orchid mantises (*Hymenopus coronatus*) have been traditionally considered a textbook example of flower mimicry for ~200 years due to their highly expanded, petal-shaped femoral lobes. However, the empirical evidence substantiating the petal-mimicry function of the femoral lobes has not been entirely conclusive.[4–6] Observational and experimental evidence suggests that these lobes do not contribute to flower mimicry for luring pollinators[6,7] and likely serve other functions.[7,8] After observing their aerial escape initiated with active jumping, we hypothesized that orchid mantises can glide and that their femoral lobes are used for gliding. Through behavioral investigations and morphological analyses, we show that orchid mantis nymphs are excellent gliders, exhibiting the shallowest gliding trajectories observed in terrestrial invertebrates.[9–13] The lobe extensions on their femoral segments are cambered airfoils, which increase the mantis projected area by ~36% and play a vital role in the aerodynamic underpinning of the observed gliding. Despite a 165-fold increase in body mass throughout ontogeny, older female mantis nymphs maintained a persistent gliding capability. We further showed a notable 40%–56% reduction in wing loading attributed to the positive size allometry of these lobes, indicating a clear promotion of gliding throughout ontogeny. This is the first documentation of gliding-adapted "leg wings" in a wingless arthropod. The evolution of such structures is potentially common among arboreal arthropods and demands a systematic re-examination.

RESULTS AND DISCUSSION

Orchid mantis nymphs are excellent gliders

We first tested whether orchid mantis nymphs (Figure 1A) could glide. We dropped 6th instar nymphs (n = 9 for each sex; STAR Methods) from a crane, 10 m above an open lawn (Figures S1A–S1E). After release, the nymphs adopted a right-side-up body posture and glided over 6.09 ± 2.25 m (mean ± SD; maximum = 9.57 m) horizontally within 3.24 ± 0.26 s prior to landing (Videos S1 and S2). The mean glide speed was 3.08 ± 0.25 m/s in the vertical and 1.88 ± 0.15 m/s in the horizontal (Figure 1B), with the effect of wind excluded (STAR Methods). The 6th instar female nymphs glided better than other wingless arthropods with an average glide angle of 52° (Figure 1C; STAR Methods), compared with a typical ~75° in gliding ants.[10]

We expected the gliding behavior to be influenced by visual cues. After preliminary experiments (STAR Methods), we tested whether gliding was directed toward or away from black surfaces in a large glide arena (Figures S1F–S1H). We found a distinct landing bias, with a significant majority of individuals (79.8%; 154 in 193 drops) landing near the black background ($G = 74.677$, $p < 0.001$; G test) (Video S3). This confirmed visually influenced steering and a potential preference for landing on dark surfaces, a potential anti-predator strategy in rainforests.

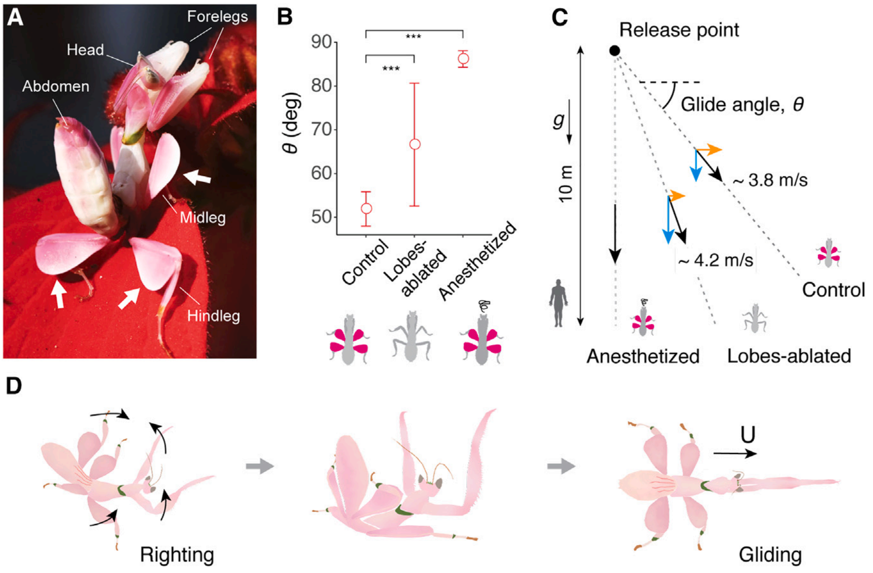

Figure 1. Orchid mantis nymphs exhibit controlled gliding

(A) An orchid mantis nymph (6th instar).

(B and C) With femoral lobes, a 6th instar nymph achieves an average glide angle (θ) of ~52° with the horizontal and glide speed (U) of ~3.8 m/s. Lobe ablation led to reduced θ and increased U, whereas anesthesia led to complete loss of the gliding capability. Values are means ± SD.

(D) Sequence of postures exhibited by a mantis nymph after release, from aerial righting (left) to gliding (right; in dorsal view). Black arrows denote dorsiflexion of legs.

See also Figures S1 and S2; Videos S1, S2, S3, and S4; and the STAR Methods.

Postural control in gliding

Intentional control of body and leg postures is required for both steering and forward gliding.[1] With the same experimental setup, we dropped anesthetized individuals and found a complete loss of gliding (Figures 1B, 1C, and S2; Video S4). From video recordings of normal orchid mantises, we identified three body-leg postures adopted during initial descent and subsequent gliding (Figure 1D): (1) immediately after release, the mantis rapidly adopted a stereotypic posture, elevating abdomen and legs dorsally, presumably inducing aerodynamic instability to correct dorsoventral orientation.[14] (2) Subsequently, during the initiation of gliding, the mantis unfolded its abdomen and extended its mid and hind legs laterally, imposing the petal-shaped femoral lobes to the vertically upward incidental flow. (3) Last, the mantis extended its fore-legs in alignment with the abdomen and maintained this posture during gliding.

Femoral lobes enhance gliding

To determine the importance of femoral lobes to gliding, we tested gliding in 6th instar nymphs (N = 11) with their femoral lobes ablated (Figures S2A–S2D). Lobe ablation led to a reduced gliding capability. The horizontal distances traveled reduced to 4.08 ± 2.39 m, ~33% shorter than in the control group (6.09 ± 2.25 m; $t = -2.28$, $p = 0.015$). Also, the glide angle averaged 67°, compared with 52° in intact individuals. The femoral lobes thus contribute to lift generation during descent and play a key role in orchid mantis nymphs gliding ability.

Morphology of femoral lobes

The morphological examination of orchid mantis' femora revealed they are ventrally cambered. Cross sections showed that the camber structure was anteroposteriorly asymmetric, and the thickness of exoskeletal lobes ranged from 0.03 to 0.10 mm, extending in anterior and posterior directions with a greater posterior size (Figures 2A and S3).

The camber ratio ranged from 8% to 12%, with the maximum deviation from chord line located at ~38% of the chordwise position. This camber ratio falls within the range of many airfoils found in flying and gliding vertebrates (e.g., bird wings, 10%–20%; flying lizard membrane, ~9%; flying squirrel patagium, ~14%).[15–17] Notably, these mantis' femur segments have a corrugated profile on both dorsal and ventral surfaces, with the leg hemocoel forming a thickened section at ~20% chord length from the leading edge. Such configuration is distinct from other biological airfoils with relatively uniform thickness (e.g., insect wings) or smooth profile (e.g., bird wings).

Ontogenetic augmentation of femoral lobes

As the mantis nymphs grew in size, the femoral lobes also became rounder and disproportionately increased in area (Figures 2B and 2C). The lobe area increased continuously throughout the whole nymphal stage, until an abrupt reduction occurred when the mantis reached adulthood. In the last nymphal stage (6th for males and 8th for females), the combined area of all femora covered a remarkable ~30% and ~36% of the whole-mantis projected planform area (A_{tot}) in males and females, respectively.

We evaluated the functional importance of femoral size allometry by calculating wing loading (p_b, with b representing "body"), which indicates the aerodynamic pressure experienced by the mantis during equilibrium gliding. This calculation relies on the projected area of the entire mantis (A_{tot}) and is expressed as $p_b = mg/A_{tot}$, with m representing mass and g denoting gravitational acceleration (STAR Methods). An increase in the lobes' relative area should reduce wing loading. Integrating the allometric scaling of body mass and planform area throughout nymphal stages (Figure S4), we developed a power-law scaling model and showed that the reduction of wing loading (Δp_b) increased with the relative area of lobed femur segments (r_L) and body size (L) (Figure 2D). Overlaying the ontogenetic trajectories of r_L onto a landscape of Δp_b, an increasing effect of wing loading reduction was evident in both sexes, reaching 28%–36% reduction in late instars.

For each nymph, the total area of their four lobed femora contributed a remarkable 21%–36% of the total planform area, contrasting with the lack of extensions in other gliding arthropods (e.g., gliding ants and spiders). In a gliding-related morpho-space defined by body size and relative area of gliding-adapted flat extensions, the orchid mantis nymphs

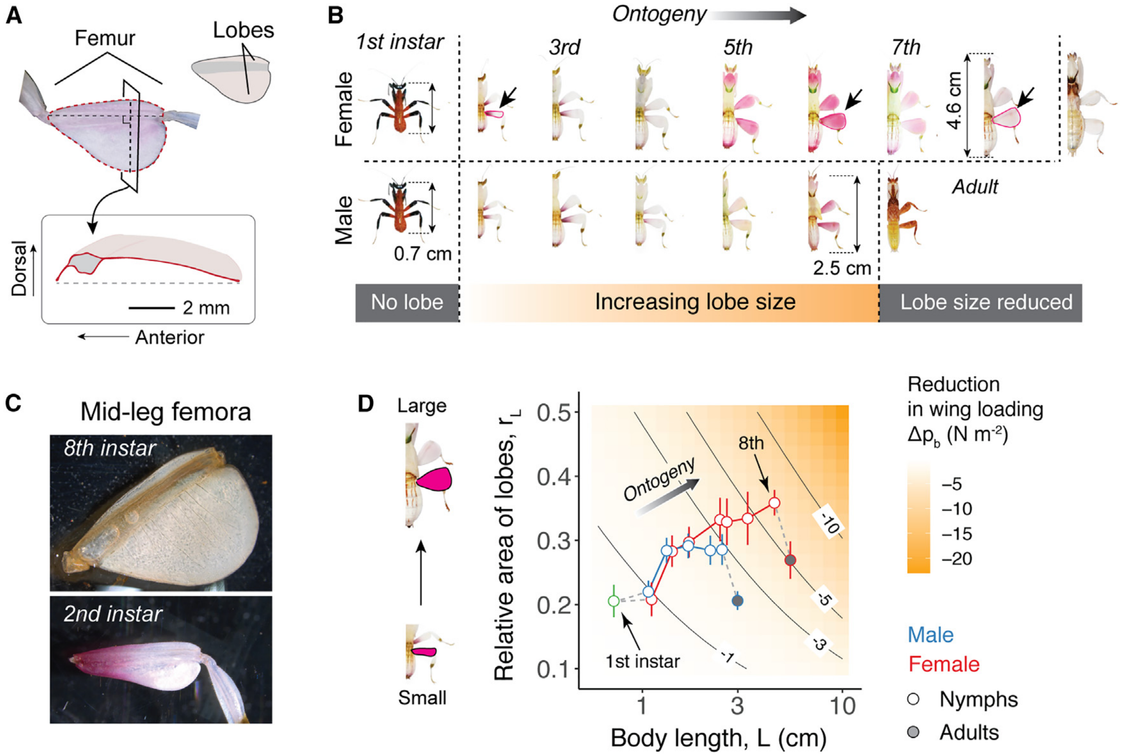

Figure 2. Femoral morphology and wing loading reduction by femoral lobes during ontogeny

(A) Femur segments are ventrally cambered and anteroposteriorly asymmetric, with a posterior lobe larger than the anterior one. Inset shows the cross-section sampled at 75% femur length from the basal end in 8th instar female (Data S1 at https://doi.org/10.17632/ggsxps2v6f.1).

(B) Ontogenetic sequences in both sexes (wings ablated in adults for clarity), showing the disproportionate increase of femoral lobe size (body sizes along ontogeny not in the same scale).

(C) Older nymphs have rounder femoral lobes.

(D) Ontogenetic increases in femoral area effectively reduce the mantises' wing loading. Values are means ± SD. See Data S2 (https://doi.org/10.17632/ggsxps2v6f.1) for detail.

See also Figure S3 and the STAR Methods.

characterize unique positions by laying between other wingless gliding arthropods,[10,13] gliding salamanders,[18] and gliding vertebrates with large areas of membranes or webbing (Figure 4A).

Ontogeny of gliding capability

Orchid mantis nymphs' body mass underwent a dramatic 165-fold increase in females (from 6.2 ± 0.8 mg in the 1st instar to 0.99 ± 0.20 g in 8th instar) and 24-fold in males (0.18 ± 0.04 g in 6th instar) (Figure S4). With isometric scaling, larger gliding animals experience a proportionally higher aerodynamic loading compared with smaller animals and demand a greater equilibrium glide speed; they likely fall over a greater distance before reaching equilibrium speed and thus exhibit reduced glide index (i.e., increased average glide angle). A positive allometry of body mass leads to a reduction in average glide angle, as shown in flying lizards,[19] gliding ants,[10] and spiders.[13] For wingless arthropod nymphs, ontogenetic increases in body size and mass should also lead to a positive allometry of wing loading and a glide angle reduction. This can be overcome by developing more aerodynamic surfaces. Is the ontogenetic augmentation of orchid mantis' femoral lobes an adaptation for gliding with larger size? If the femoral lobes were ineffective in helping glide, we would at least expect an ontogenetic reduction in glide angle.

We tested this hypothesis by dropping different-aged nymphs from the 10-m crane. In female nymphs, we found relatively persistent glide distances (4–6 m) across age groups (Figure 3A), whereas mean glide speed increased from ~2 m/s in 1st instar nymphs to ~4 m/s in 8th instar females (Figures 3B, 3C, and 3E). The increases in glide speed correspond with an increase in aerodynamic force to offset body weight.[3] With increasing wing loading, the average glide angle remained between 60° and 70° in females but increased more steeply in males (Figures 3D and 3E). This showed sex-specific allometries in gliding reduction, with a persistent gliding capability in female nymphs despite a two-order of magnitude increase in wing loading.

Orchid mantis nymphs exhibited an intermediate wing loading (2.2–11.9 N m^{-2}) between those of wingless gliding arthropods and vertebrates (Figure 4B). Compared with gliding ants and spiders, orchid mantis nymphs also showed negative allometries of glide index (with sex-specific slopes), but they glided better at equivalent body masses (Figure 4C). In particular, female mantis nymphs (glide index 0.4–0.6) traveled 20%–50% farther than gliding spiders and 50%–200% farther than gliding ants of similar masses. Despite their gliding abilities, wingless gliding arthropods are limited to a glide index < 1 (with average glide angle > 45°).

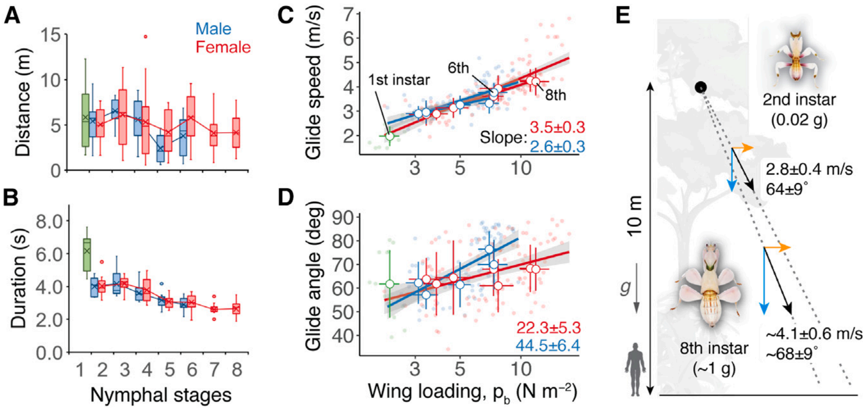

Figure 3. Ontogeny of gliding in orchid mantis nymphs

(A and B) Despite increases in body size and mass, the horizontal distance traveled (A) did not decrease, whereas duration (B) declined. Boxplots show 25th to 75th percentiles, median (lines), mean (crosses), maximum and minimum values (whiskers), and outliers (dots).

(C) Mean glide speed increased with increasing wing loading.

(D and E) Mean glide angle increased in male nymphs but was relatively consistent in females. Values are means ± SD in (C) and (D); trend lines represent linear regressions with $\log_{10}$-transformed (p_b); shades representing SEM. (E) Increase in glide speed without reduction of glide angle in female nymphs, comparing 2nd and 8th instars. Arrow size represents the relative magnitude of velocity components based on mean values. See Data S2 (https://doi.org/10.17632/ggsxps2v6f.1) for details.

See also Figure S4.

Leg wings and gliding in orchid mantises

We showed that wingless orchid mantis nymphs are remarkable gliders owing to their femoral lobes acting as wing-like structures. Why do orchid mantises glide in the first place? They are presumably subject to the same selective pressure for aerial escape and dispersal as other arboreal invertebrates,[2,20] and they may also rely on gliding to access hunting territories.

Lobe-ablation experiments and preliminary characterization of femoral lobe morphology revealed a new type of biological airfoil—non-flapping "leg wings" derived from exoskeleton and used in gliding. The ventrally cambered shape likely facilitates lift generation during gliding,[21] but its aerodynamic properties require more detailed examination, especially concerning the contributions of the corrugated camber profile, body kinematics, and leg postures. The aerodynamic mechanism of these lobed femora may vary with their size, shape, and gliding performance at different air speeds. For example, as female mantises progressed from the 1st to the 8th instar, the Reynolds number increased by over 300 times (from ~70 to 2.2×10^3), whereas the increase in body length was just ~14 times (from ~9×10^2 to 1.3×10^4). The lobe-ablated mantises also performed well in gliding compared with other wingless gliding arthropods, suggesting substantial aerodynamic capability conferred by the body and legs, especially a flat, broad abdomen. The expanded femoral lobes may be particularly important to reducing wing loading in larger nymphs. This hypothesis may be partially supported by the gliding capability of the 1st instar orchid mantis nymphs and gliding ants,[10] which have similar body mass and lack extensions on body and legs.

We further showed that the expansion of femoral lobes along ontogeny reduced wing loading and improved gliding. This likely corresponds with a sustained selective pressure for gliding throughout the nymphal stage. Compared with males, the persistent gliding capability in females may help compensate for the relatively higher energetic cost of dispersal and higher predation risk associated with larger body sizes.[22] The decrease in relative lobe size from the last nymphal stage to adulthood (Figure 2) could be indicative of a reduced need for gliding because adults possess fully developed wings and are capable of powered flight.

Evolution of gliding-adapted structures in wingless arthropods

To our knowledge, this is the first documentation of an arthropod leg wing used for gliding. The lack of reports of such structures may be partly attributed to the long-term misinterpretation of their function. Among terrestrial arthropods, although visual mimicry is frequently interpreted as the main function of flat structures, the actual utility and underlying evolutionary motivation can only be justified through empirical experiments. For example, orchid mantis femoral lobes, although interpreted as flower mimics for ~200 years, do not contribute to luring pollinating preys[6] but facilitate gliding.

We speculate that a substantial diversity of flat exoskeletal structures found on body and appendages in terrestrial arthropods may contribute to gliding, especially among hemimetabolous insects, such as leaf insects, stick insects, mantids, and leaf-footed bugs.[23–25] Many of these insects are arboreal, undergo relatively long nymphal stages, and grow into large nymphs, thus possibly being subject to selective pressures for gliding.[24]

Unlike vertebrates' collapsible membranes and webbings[26–29] and insects' winglets,[30] rigid exoskeletal extensions on arthropod legs cannot change shape or size during aerial performances and have limited flexibility and mobility. Although larger lobes may be advantageous for improved gliding, they could potentially have adverse effects on survivorship due to prolonged molting, increased risk of molting failure, hindered locomotion, or increasing the mantis conspicuousness to predators.[19] Therefore, the evolution of flat extensions on arthropod body and legs could be subject to functional tradeoffs, which deserves further investigation.

Future work should study three-dimensional glide trajectories in orchid mantises to reveal mid-air maneuvers and forward gliding performance toward the end of trajectories. Considering the scarcity of gliding allometry data (Figure 4C), it becomes crucial to conduct further investigations into the ontogeny of

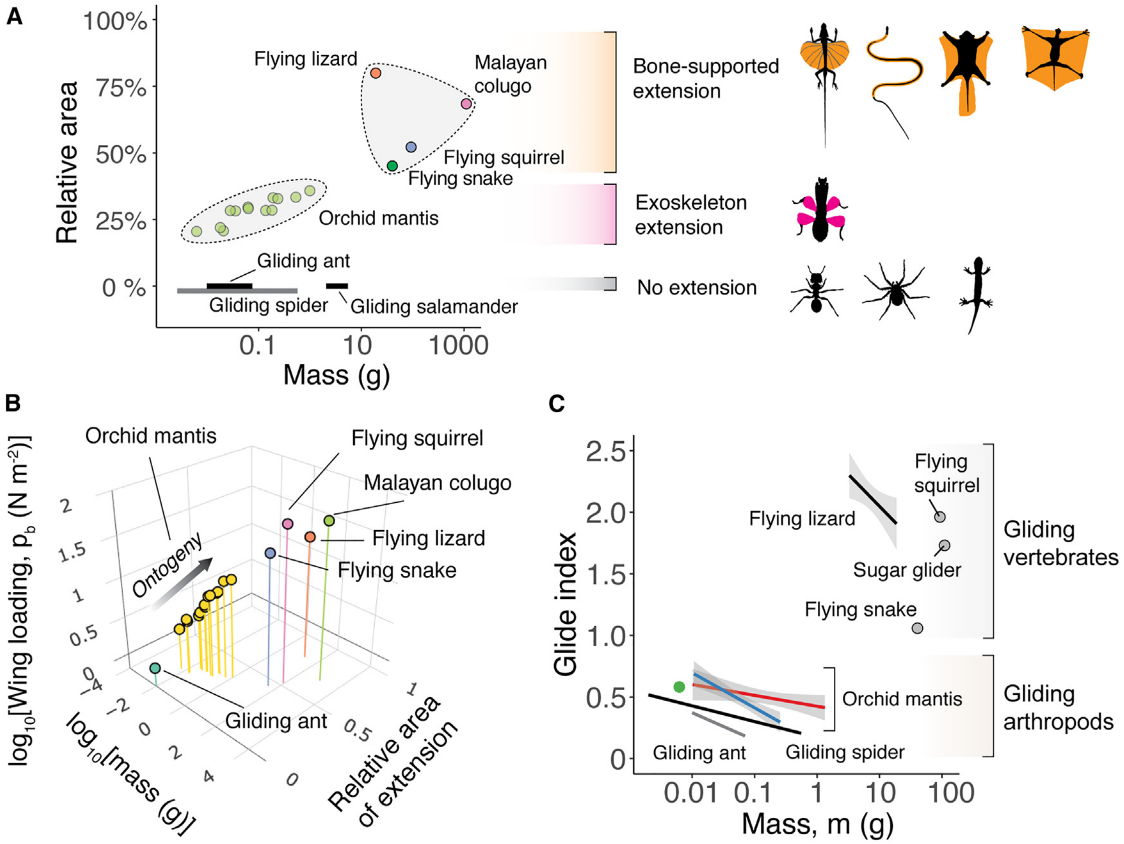

Figure 4. Comparisons of gliding morphology and gliding capability between gliding animals

(A) Relative areas of extended surfaces (relative to the animal's projected planform area) against whole-animal mass. Orchid mantis' femoral lobes provide a smaller surface area compared with vertebrate gliders' membranes or webs (orange highlight), but they stand out compared with gliding animals without obvious extensions.

(B) Comparison of wing loading (p_b) between orchid mantis nymphs, gliding ants, and gliding vertebrates within a morpho-space defined by mass and the relative area of extensions. For orchid mantis, points represent instar-specific means of both sexes. Morphology data of other taxa were aggregated based on availability (Data S3 at https://doi.org/10.17632/xzx5srxf8k.1).

(C) Glide index versus mass in different gliding animals. Glide index allometries in wingless arthropods (lower left) and vertebrates (upper right). Slopes in orchid mantis (female, −0.09 ± 0.05, $p < 0.0001$; males, −0.28 ± 0.06, $p < 0.001$) are comparable to those of gliding ants (−0.097)[10] and spiders (−0.164).[12,13] Orchid mantis nymphs traveled farther per unit descent than the other two arthropods of similar mass. Lines represent linear regressions for all nymphal stages, excluding the first; shades represent SEM. Vertebrate data were obtained from the literature.[3,19]

gliding and gliding kinematics, particularly in large wingless arthropods. Such research is essential to comprehending how gliding-adapted structures evolve in different clades and body sizes.

STAR★METHODS

Detailed methods are provided in the online version of this paper and include the following:

- KEY RESOURCES TABLE
- RESOURCE AVAILABILITY
  - ○ Lead contact
  - ○ Materials availability
  - ○ Data and code availability
- EXPERIMENTAL MODEL AND STUDY PARTICIPANT DETAILS
- METHOD DETAILS
  - ○ Morphometrics
  - ○ Outdoor dropping experiments
  - ○ Evaluation of visual cues used in gliding
- QUANTIFICATION AND STATISTICAL ANALYSIS
  - ○ Outdoor dropping experiments
  - ○ Evaluation of visual cues used in gliding
  - ○ The effectiveness of wing loading reduction by femoral lobes
  - ○ Allometric scaling of wing loading in ontogeny

SUPPLEMENTAL INFORMATION

Supplemental information can be found online at https://doi.org/10.1016/j.cub.2023.11.003.

ACKNOWLEDGMENTS

We thank two anonymous reviewers and Rui-Chang Quan for suggestions, and we thank Xi-Yuan Ni, Nan-Wei Yi, Yi-Rong Wang, Shao-Xiang Ge, Chu

Jiang, Bai-Lu Chen, Qin Li, and Yue Yu for experimental assistance. We thank Christian Brown for data sharing, Chao Wu for discussion, and Sheng Li and Xiao-Jin Pei for providing photographs. This study was funded by the Hundred Talents Program of Chinese Academy of Sciences (292022000040); the National Natural Science Foundation of China (31970425); the Natural Science Foundation of Yunnan Province (202001AV070013), China; the West Light Foundation of the Chinese Academy of Sciences (2021000018), China; and the Ten Thousand Talent Plans for Young Top-notch Talents of Yunnan (20200000099), China.

AUTHOR CONTRIBUTIONS

Conceptualization, Z.C., X.Z., J.-X.L., and Y.Z.; methodology, X.Z., Y.Z., J.-X.L., and Z.C.; investigation, X.Z., J.-X.L., Z.C., B.D., and L.Y.; visualization, Y.Z., X.Z., Z.C., J.-X.L., and T.C.-D.; funding acquisition, Z.C.; project administration, Z.C.; supervision, Z.C. and Y.Z.; writing – original draft, X.Z., Y.Z., Z.C., and J.-X.L.; writing – review & editing, all authors.

DECLARATION OF INTERESTS

The authors declare no competing interests.

Received: July 30, 2023
Revised: September 24, 2023
Accepted: November 2, 2023
Published: November 29, 2023

REFERENCES

1. Dudley, R., Byrnes, G., Yanoviak, S.P., Borrell, B., Brown, R.M., and McGuire, J.A. (2007). Gliding and the functional origins of flight: biomechanical novelty or necessity? Annu. Rev. Ecol. Evol. Syst. *38*, 179–201.
2. Dudley, R., and Yanoviak, S.P. (2011). Animal aloft: the origins of aerial behavior and flight. Integr. Comp. Biol. *51*, 926–936.
3. Socha, J.J., Jafari, F., Munk, Y., and Byrnes, G. (2015). How animals glide: from trajectory to morphology. Can. J. Zool. *93*, 901–924.
4. O'Hanlon, J.C., Li, D., and Norma-Rashid, Y. (2013). Coloration and morphology of the orchid mantis *Hymenopus coronatus* (Mantodea: Hymenopodidae). J. Orthop. Res. *22*, 35–44.
5. O'Hanlon, J.C. (2016). Orchid mantis. Curr. Biol. *26*, R145–R146.
6. O'Hanlon, J.C. (2014). The roles of colour and shape in pollinator deception in the orchid mantis *Hymenopus coronatus*. Ethology *120*, 652–661.
7. Siedlecki, M. (1917). Spadochronowy lot niektórych owadów – Der Fallschirmflug einiger Insekten. Bull. Int. Acad. Pol. Sci. Lett. *ser B*, 230–256.
8. Zhao, X., Liu, J.X., and Chen, Z.Q. (2023). The orchid mantis exhibits high ontogenetic colouration variety and intersexual life history differences. Evol. Ecol. *37*, 569–582.
9. Yanoviak, S.P., Kaspari, M., and Dudley, R. (2009). Gliding hexapods and the origins of insect aerial behaviour. Biol. Lett. *5*, 510–512.
10. Yanoviak, S.P., Dudley, R., and Kaspari, M. (2005). Directed aerial descent in canopy ants. Nature *433*, 624–626.
11. Yanoviak, S.P., Munk, Y., Kaspari, M., and Dudley, R. (2010). Aerial manoeuvrability in wingless gliding ants (*Cephalotes atratus*). Proc. Biol. Sci. *277*, 2199–2204.
12. Yanoviak, S.P., Munk, Y., and Dudley, R. (2011). Evolution and ecology of directed aerial descent in arboreal ants. Integr. Comp. Biol. *51*, 944–956.
13. Yanoviak, S.P., Munk, Y., and Dudley, R. (2015). Arachnid aloft: directed aerial descent in Neotropical canopy spiders. J. R. Soc. Interface *12*, 0534.
14. Zeng, Y., Lam, K., Chen, Y., Gong, M., Xu, Z., and Dudley, R. (2017). Biomechanics of aerial righting in wingless nymphal stick insects *Extatosoma tiaratum*. Interface Focus *7*, 20160075.
15. Rader, J.A., Hedrick, T.L., He, Y., and Waldrop, L.D. (2020). Functional morphology of gliding flight II. Morphology follows predictions of gliding performance. Integr. Comp. Biol. *60*, 1297–1308.
16. Bishop, K.L. (2006). The relationship between 3-D kinematics and gliding performance in the southern flying squirrel, *Glaucomys volans*. J. Exp. Biol. *209*, 689–701.
17. Khandelwal, P.C., and Hedrick, T.L. (2022). Combined effects of body posture and three-dimensional wing shape enable efficient gliding in flying lizards. Sci. Rep. *12*, 1793.
18. Brown, C.E., Sathe, E.A., Dudley, R., and Deban, S.M. (2022). Gliding and parachuting by arboreal salamanders. Curr. Biol. *32*, R453–R454.
19. McGuire, J.A., and Dudley, R. (2005). The cost of living large: comparative gliding performance in flying lizards (Agamidae: *Draco*). Am. Nat. *166*, 93–106.
20. Khandelwal, P.C., Ross, S.D., Dong, H., and Socha, J.J. (2023). Convergence in gliding animals: morphology, behavior, and mechanics. In Convergent Evolution: Animal Form and Function (Springer), pp. 391–429.
21. Sunada, S., Takashima, H., Hattori, T., Yasuda, K., and Kawachi, K. (2002). Fluid-dynamic characteristics of a bristled wing. J. Exp. Biol. *205*, 2737–2744.
22. Chown, S.L., and Gaston, K.J. (2010). Body size variation in insects: a macroecological perspective. Biol. Rev. Camb. Philos. Soc. *85*, 139–169.
23. Boisseau, R.P.G.E. (2022). The Evolution of Morphological Diversity and Sexual Dimorphism in Stick and Leaf Insects (University of Montana).
24. Emberts, Z., St Mary, C.M., Howard, C.C., Forthman, M., Bateman, P.W., Somjee, U., Hwang, W.S., Li, D., Kimball, R.T., and Miller, C.W. (2020). The evolution of autotomy in leaf-footed bugs. Evolution *74*, 897–910.
25. Svenson, G.J., Hardy, N.B., Cahill Wightman, H.M., and Wieland, F. (2015). Of flowers and twigs: phylogenetic revision of the plant-mimicking praying mantises (Mantodea: Empusidae and Hymenopodidae) with a new suprageneric classification. Syst. Entomol. *40*, 789–834.
26. McGuire, J.A., and Dudley, R. (2011). The biology of gliding in flying lizards (genus *Draco*) and their fossil and extant analogs. Integr. Comp. Biol. *51*, 983–990.
27. Jackson, S.M. (2000). Glide angle in the genus *Petaurus* and a review of gliding in mammals. Mamm. Rev. *30*, 9–30.
28. Wu, W., Gao, Y.-D., Jiang, D.-C., Lei, J., Ren, J.-L., Liao, W.-B., Deng, C., Wang, Z., Hillis, D.M., Zhang, Y.-P., et al. (2022). Genomic adaptations for arboreal locomotion in Asian flying treefrogs. Proc. Natl. Acad. Sci. USA *119*, e2116342119.
29. Socha, J.J. (2011). Gliding flight in *Chrysopelea*: turning a snake into a wing. Integr. Comp. Biol. *51*, 969–982.
30. Zeng, Y., Park, S., Gonzales, C., Yom, S., Rahim, F., and Dudley, R. (2023). Beyond winglets: evolutionary scaling of flight-related morphology in stick insects (Phasmatodea). Biol. J. Linn. Soc. *140*, blad050.
31. Roeder, K.D. (1935). An experimental analysis of the sexual behavior of the praying mantis (*Mantis religiosa L.*). Biol. Bull. *69*, 203–220.
32. Brannoch, S.K., Wieland, F., Rivera, J., Klass, K.D., Olivier, B., and Svenson, G.J. (2017). Manual of praying mantis morphology, nomenclature, and practices (Insecta, Mantodea). ZooKeys *696*, 1–100.
33. Abràmoff, M.D., Magalhães, P.J., and Ram, S.J. (2004). Image processing with ImageJ. Biophotonics Int. *11*, 36–42.
34. Kandori, I., Hiramatsu, M., Soda, M., Nakashima, S., Funami, S., Yokoi, T., Tsuchihara, K., and Papaj, D.R. (2022). Long horns protect *Hestina japonica* butterfly larvae from their natural enemies. Sci. Rep. *12*, 2835.
35. Zeng, Y., Lin, Y., Abundo, A., and Dudley, R. (2015). Visual ecology of directed aerial descent in first-instar nymphs of the stick insect *Extatosoma tiaratum*. J. Exp. Biol. *218*, 2305–2314.
36. Yanoviak, S.P., and Dudley, R. (2006). The role of visual cues in directed aerial descent of *Cephalotes atratus* workers (Hymenoptera: Formicidae). J. Exp. Biol. *209*, 1777–1783.

37. R Core Team (2022). R: A Language and Environment for Statistical Computing (R Foundation for Statistical Computing).

38. RStudio Team (2022). RStudio: integrated development for R (RStudio).

39. Lüdecke, D., Ben-Shachar, M., Patil, I., Waggoner, P., and Makowski, D. (2021). performance: an R package for assessment, comparison and testing of statistical models. J. Open Source Softw. *6*, 3139.

40. Lüdecke, D. (2022). Performance: assessment of regression models performance. R package version 0.10.0.

41. Pinheiro, J., and Bates, D.; R Core Team (2022). Nlme: linear and nonlinear mixed effects models. R package version 3.1-158. https://CRAN.R-project.org/package=nlme.

STAR★METHODS

KEY RESOURCES TABLE

REAGENT or RESOURCE	SOURCE	IDENTIFIER
Deposited data		
Experimental data (Raw data, Data S1, S2, and S4–S6)	This paper	Mendeley Data: https://doi.org/10.17632/ggsxps2v6f.1
Experimental video (Videos S1, S2, S3, and S4)	This paper	Mendeley Data: https://doi.org/10.17632/bwh2nt6g4k.1
Other gliding animal data (Data S3)	Other papers (citations could be referred to Mendeley Data)	Mendeley Data: https://doi.org/10.17632/xzx5srxf8k.1
Experimental models: Organisms/strains		
Hymenopus coronatus	Indoor reared in Xishuangbanna Tropical Botanical Garden (XTBG), Yunnan, China (approx. 21° 55′ N, 101° 16′ E)	Indoor type
Software and algorithms		
R 4.2.1 in RStudio	R Core Team	https://www.r-project.org/
ImageJ 1.52	National Institutes of Health (NIH)	https://imagej.nih.gov/ij/
Adobe Photoshop 24.0.0	Adobe	https://www.adobe.com/cn/
Other		
Digital camera (Nikon D750)	Nikon	https://www.nikon.com.cn/sc_CN/
Electric balance (HZK-FA11OS; accuracy, 0.0001 g)	HUAZHI	http://www.fzhz.com.cn/index.jsp
LEICA DMC 4500 stereo microscope	Leica	https://www.leica.com/
GoPro Hero 8	GoPro	https://gopro.com/zh/cn/
Anemometer AR816$^+$	SMART SENSOR	https://www.smartsensor.cn/

RESOURCE AVAILABILITY

Lead contact

Further information and requests should be directed to and will be fulfilled by the lead contact, Zhanqi Chen (chenzhanqi@xtbg.ac.cn).

Materials availability

This study did not generate new unique reagents.

Data and code availability

- All the original data are available through the Mendeley data repository: https://doi.org/10.17632/ggsxps2v6f.1.
- This paper does not report original code.
- Any additional information required to reanalyze the data reported in this work paper is available from the lead contact upon request.

EXPERIMENTAL MODEL AND STUDY PARTICIPANT DETAILS

The orchid mantis *Hymenopus coronatus* Olivier, 1792 (Insecta: Mantodea) is an arboreal species native to Southern China and Southeast Asia.[5] The wingless nymphs of this species are visually stunning with foliaceous lobes on their femoral segments of mid- and hind-legs[4,5] (Figure 1A). For this reason, they have been interpreted as a textbook example of flower-mimicry for ~200 years. However, more recent evidence suggests that these lobes do not contribute to flower mimicry for luring pollinators[6] and likely serve other functions.[8] Throughout the majority of wingless nymphal stages (around five months), they are diurnally active and perch on open surfaces of canopies in tropical rainforests.[5] After observing these mantis nymphs' aerial escape initiated with active jumping, we hypothesized that their femoral lobes are used for gliding. We then investigated their gliding capability and the role of femoral lobes in captive-reared individuals under controlled conditions.

All experimental mantises were house-reared in Xishuangbanna Tropical Botanical Garden (XTBG, 21° 55′ N, 101° 16′ E; within the natural distribution of the orchid mantis), Yunnan, China.[8] The parental mantises were collected in or near XTBG. We determined the sex of each individual (except 1st instar nymphs) based on the slightly upturned edge of the last sternum and fewer coxosternites in females.[31],[32]

METHOD DETAILS

Morphometrics

For each experimental individual, we collected morphometrics data within 6 hours after dropping experiments and before feeding. Individual mantises were first anesthetized by ethyl acetate (99%) for 5 – 10 minutes within a sealed plastic box (15 × 10 × 5 cm). To obtain projected planform areas of body and leg segments, anesthetized mantises were laid dorsoventrally on a flat surface with their legs fully extended (Figure S3A). Afterward, two-dimensional images were taken from above using a digital camera (Nikon D750). The projected planform areas of the whole-mantis (A_{tot}) and of all femurs (A_{femur}) were measured using ImageJ (version 1.52; Figure S3B).[33] The relative area of femur segments was calculated as: $r_L = \frac{A_{femur}}{A_{tot}}$. Whole-mantis mass ($m$) was measured using an electric balance (HZK-FA11OS; accuracy, 0.0001 g). Measurements for each individual were completed within 10 minutes, after which the mantis was returned to the rearing box. For all the wingless nymphs, the wing loading for the combination of body and legs was calculated as:

$$p_b = \frac{mg}{A_{tot}} \qquad \text{(Equation 1)}$$

where g is gravitational acceleration.

We also sampled the cambered profile and aspect ratio of femurs in freshly euthanized mantises. For a conservative evaluation of the camber profile, we sampled the cross-sections of femurs at 75% length from the basal end (Figures S3B–S3D). This choice was made independently of any prior insights into leg-flow configuration. We selected this specific location because it encompasses the broadest chord section, allowing for a reliable and reproducible result that can be compared to other research on wing aerodynamics. The camber ratio was calculated as the ratio between the maximum deviation of the camber line with respect to the chord line. Based on images of femur taken in dorsal view, the aspect ratio of femora was calculated as $AR = L_{femur}^2 / A_{femur}$, where L_{femur} is the length of femur segment (Figures S3E and S3F).

Outdoor dropping experiments

We conducted outdoor dropping experiments under semi-natural condition in XTBG in Jan. and Apr. 2022 (Figures S1A–S1C). A large crane was recruited with the operating platform fixed at ten meters above ground (Figure S1D), which was measured between the release point and the ground using a cloth tape. To record the landing points, we established a coordinates system on the ground, with the origin point determined using a plumbline hung from the release point (Figure S1E). Each experimental mantis was first transferred to an acrylic sheet (6 × 8 cm) attached to a pole. Next, the experimenter initiated the drop by stimulating a startle response or quickly flipping the sheet. After each drop, the coordinates of the landing point were recorded and later converted to the horizontal gliding distance. The glide duration was calculated as the average of three independent stopwatch recordings made by three experimenters standing on the ground. We also recorded sample videos using a sport camera (GoPro Hero 8, GoPro) facing downward (Videos S1 and S2). Body and leg postures after dropping were obtained from video frames for the schematic diagrams (Figure 1D).

During the experimental time (14:00 - 17:00), we sampled the wind speed three times each hour, each time for three minutes, using an anemoscope (SMART SENSOR AR816$^+$) at 2.5 m above ground. The wind speed ranged 0 - 1.2 m/s and was 0.04 ± 0.14 m/s (mean ± S.D.), significantly lower than the mean horizontal speed recorded in gliding mantis nymphs (0.5 – 1.6 m/s; Data S2).

Glide index was calculated as the ratio of horizontal gliding distance and height lost prior to landing. The glide angle was calculated as $\theta_{min} = \tan(d_v / d_h)$, where d_v and d_h are travelled distances in vertical and horizontal directions, respectively. This is a conservative model omitting the height loss during the initial descent (i.e., from release to the start of gliding). The mean vertical speed was calculated as $\overline{U_v} = \frac{d_v}{t_L}$ and mean horizontal speed as $\overline{U_h} = \frac{d_h}{t_L}$, where t_L is the total time expenditure of aerial travel; then the mean glide speed $\overline{U}$ was calculated as the resultant of $\overline{U_v}$ and $\overline{U_h}$.

Experiment 1: the importance of intentional postural control

To test our hypothesis that intentional body and leg postural control is essential for gliding in orchid mantis nymphs, we dropped ten anesthetized 8th instar females using the same method as above and compared the performance with that of ten conscious individuals (control group). Mantis nymphs were anesthetized with 5-minute exposure to ethyl acetate (99%) shortly before experiments.

Experiment 2: the importance of femoral lobes

We examined how the ablation of femoral lobes would impact gliding capability using 6th instar nymphs. Twenty-nine individuals were divided into two groups: (a) a control group (n = 18 individuals) and (b) a treated group with femoral lobes ablated (n = 11). We modified the method of removing caterpillar horns[34] to ablate the femoral lobes. Specifically, we first anesthetized the mantises using ethyl acetate (99%), and then heated the tips of forceps with an alcohol burner until they turned red. The heated forceps were used to pinch and burn the extended femoral lobes as much as possible without damaging the leg joints (Figures S2A and S2B).

The ablated lobe area (0.35 ± 0.16 cm^2) accounted for 16.75% of total body area in projected planform (2.09 ± 0.68 cm^2) and 34.82% of the whole femur area (0.99 ± 0.35 cm^2). After lobe-ablation, the nymphs were reared as usual for one week before the gliding experiments. Most lobe-ablated mantises survived and molted as normal (Figures S2C and S2D).

Experiment 3: ontogenetic variation of gliding capability

A total of 177 nymphs from 1^{st} to 8^{th} instar were used in this experiment (Data S5 for detailed sample sizes). The sex of 1^{st} instar nymphs was not identified given the lack of sexual dimorphism.

Evaluation of visual cues used in gliding

In preliminary experiments, we dropped 1^{st} (n = 9) and 2^{nd} (n = 6) instar nymphs from 2 m above ground and 50 cm away from vertically oriented black stripes (15 cm wide) with a white background, a visual pattern that attracted gliding stick insect nymphs (body length, ~1.7 cm; mass, ~25 mg).[35] However, the mantis nymphs did not show significant landing preference. From video recordings, we noticed that they steered with relatively large turning radii and speculated that they required a larger space to steer and relied on different visual cues to land as compared to gliding ants[36] or gliding stick insect nymphs.[35]

We prepared an indoor gliding arena (ca. 15 ×15 ×15 m) in the hall of the administrative building in XTBG. We hung a black cloth (5 × 4.2 m) four meters away from the dropping point as the visual cue and covered the floor with another black cloth (8 × 8 m) (Figures S1F–S1H). Individual mantises were released from 4.2 m above the center of the black cloth on the floor. In total, 193 nymphs from the 1^{st} to 6^{th} instar were used in this experiment, including 1^{st} instar nymphs (n = 30), 2^{nd} instar nymphs (n = 35), 3^{rd} instar nymphs (n = 25), 4^{th} instar nymphs (n = 34), 5^{th} instar nymphs (n = 34) and 6^{th} instar nymphs (n = 35).

We recorded landing at the closer side if the shortest distance between the landing point and the vertical black cloth plane was < 4 m, otherwise recorded as landing at the further side.

QUANTIFICATION AND STATISTICAL ANALYSIS

Outdoor dropping experiments

All statistical analyses were carried out by R 4.2.1[37] in RStudio.[38] Model assumptions were checked with the R package "performance",[39,40] and generalized least-squares (gls) analyses were performed using R package "nlme".[41]

Experiment 1: the importance of intentional postural control

Gliding performance of the control group and anesthetized group were compared using analysis of variance (ANOVA).

Experiment 2: the importance of femoral lobes

Gliding performance of the control group and lobe-ablated group were compared using analysis of variance (ANOVA).

Experiment 3: ontogenetic variation of gliding capability

For these 1st - 8th instar nymphs, intersexual comparisons of gliding-related morphology and gliding performance were made for each instar stage using simple linear regression models (lm) when all model assumptions were satisfied or generalized least square regression model (gls) when variance homogeneity assumption of lm failed (Data S3 and S5). Ontogenetic variation of gliding performances between two sexes were checked by lm model with data from 2^{nd} – 6^{th} instar male nymphs and 2^{nd} – 8^{th} instar female nymphs.

Evaluation of visual cues used in gliding

G-test was applied to analyze whether the mantises exhibited landing preference, with the null assuming no significance bias of landing preference (i.e., 1 : 1).

The effectiveness of wing loading reduction by femoral lobes

The relative area of femoral lobes (r_L) increased through ontogeny and lowered wing loading (p_b) (Figure 2D). We want to develop a simplified model, based on power-law scaling models, to help visualize and quantify the significance of lobe expansion. This model can also be used for ontogenetic expansion of flat surfaces found in wingless arthropods.

First, given the insignificant sexual differences in mass allometry (Figure S4A), we expressed mass (m) as a power-law function of body size (L):

$$m = a_1 L^{b_1} \tag{Equation 2}$$

Next, we obtained a power-law scaling model for the whole-mantis projected planform area (A_{tot}; Figure S4B), which was expressed as

$$A_{tot} = a_2 L^{b_2} \tag{Equation 3}$$

For a control model considering a mantis without femoral lobes, the total area is $A_{bl} = A_{tot}(1 - r_L)$. The control wing loading without lobes is:

$$p'_b = \frac{mg}{A_{bl}} = \frac{mg}{A_{tot}(1 - r_L)} \qquad \text{(Equation 4)}$$

Combining Equations 2, 3, and 4, we obtain the reduction in wing loading (Δp_b) expressed with respect to L and r_L:

$$\begin{aligned} \Delta p_b &= p_b - p'_b \\ &= \frac{mg}{A_{tot}}\left(\frac{-r_L}{1 - r_L}\right) = \frac{a_1}{a_2} g L^{b_1 - b_2}\left(\frac{-r_L}{1 - r_L}\right) \end{aligned} \qquad \text{(Equation 5)}$$

Equation 5 was used to generate the landscape of Δp_b with respect to L and r_L (Figure 2D).

Allometric scaling of wing loading in ontogeny

We want to derive a scaling model to demonstrate why larger gliding animals have greater wing loading (i.e., aerodynamic pressure exerted onto the animal during equilibrium gliding). Assuming the geometry of body plan is conserved (i.e., isometry), the body mass (m) and the project area (A_{tot}) would scale with body size (L) as $m \propto L^3$ and $A_{tot} \propto L^2$, respectively. Consequentially, wing loading would linearly increase with body size: $p_b \propto m A_{tot}^{-1} \propto L$. This shows that wing loading increases with body size. For larger animals gliding at equilibrium state, a greater glide speed is needed to generate sufficient vertical force to offset body weight. More importantly, larger animals may experience longer falling distances before reaching an equilibrium glide phase, which may on average reduce the horizontal distance travelled per vertical height loss. For example, larger flying lizards are characterized by larger wing loading and higher glide angle than smaller individuals.[19]